Cartographic Modeling for Spatiotemporal Analysis of the Summer Urban Heat Island: Kirkuk City as a Case Study

Saif Sultan Ahmed Al AKeedi[1], Prof. Dr. Ahmad Abdulghafour[2]

[1]Department of Geography and Geographic Information Systems (GIS), College of Arts, University of Tikrit, Iraq, SS240009prt@st.tu.edu.iq

[2]Department of Geography and Geographic Information Systems (GIS), College of Arts, University of Tikrit, Iraq, seed.ahmed76@tu.edu.iq

Abstract

This study aims to conduct a spatial analysis of the urban heat island (UHI) phenomenon across the neighborhoods of Kirkuk City, along with a temporal analysis spanning two distinct periods (2008 and 2025) during the summer season. This is achieved through illustrative maps that demonstrate the variations in concentration levels and the transitions that occurred, utilizing ArcGIS software. The core problem of the study highlights the impact of climate change on exacerbating the urban heat island phenomenon within the city, particularly during the summer. To fulfill the study's objectives, satellite imagery from Landsat was utilized, specifically band 6 of Landsat 7 and band 10 of Landsat 8. The study is structured into three main sections: the first section covers the theoretical framework; the second section addresses the concept of cartographic modeling alongside the requirements and procedural steps for deriving Land Surface Temperature (LST) and heat islands; while the third section encompasses the spatiotemporal analysis of the summer surface urban heat island (LST) within the study area. The study reached several key conclusions, most notably that the surface urban heat island in Kirkuk City is primarily located on the outskirts of the city, with its highest concentration during the summer of 2008 observed in the eastern and southern sectors. By 2025, this phenomenon expanded to cover most parts of the city as well as scattered interior pockets. Furthermore, the neighborhoods of Darwaza and Al-Amal Al-Sha'abi recorded the highest temperatures. This spike is attributed to the presence of the "Eternal Fire" in those locations, alongside the topographic elevations in the eastern and northern parts of the study area. The study also demonstrated that the impact of the urban heat island in Kirkuk City intensified significantly in 2025 compared to 2008 during the summer season. This intensification is driven by accelerated urban expansion, the recession of vegetation cover, and the overarching factor of climate change, which has further compounded the urban heat island phenomenon in Kirkuk City.

- **Keywords: Remote Sensing, Geographic Information Systems (GIS), Urban Heat Island (UHI), Models, Climate Change.**
- *This research is extracted from a master's thesis.*

Introduction

The process of modeling and designing maps for urban heat islands is considered one of the most critical tools for understanding the thermal variations witnessed across the study area. While numerous studies examine the phenomenon of urban heat islands of all types, this research specifically focuses on Surface Urban Heat Island (SUHI). This particular type stands out as one of the most vital and prevalent subjects in contemporary environmental and climatological studies. Accordingly, this study concentrates on extracting temporally and spatially varying temperatures across the neighborhoods of Kirkuk City. This is executed utilizing Landsat satellite imagery—specifically from Landsat 7 and Landsat 8, focusing on bands 6 and 10—during the summer season across two distinct periods (2008 and 2025). The primary objective is to monitor the spatiotemporal patterns of the heat island associated with the variations in land use within the study area.

Section One: Theoretical Framework

First: Research Problem

The research addresses the core problem of the study through a series of specific inquiries, formulated as follows:

1. Does climate change exert a direct impact on exacerbating the summer urban heat island phenomenon in Kirkuk City?
2. Do urban heat islands exhibit spatial and temporal variations across Kirkuk City?
3. What is the role of remote sensing and Geographic Information Systems (GIS) technologies in monitoring and mapping cognitive perceptions regarding the distribution of the urban heat island?

Second: Research Hypothesis

1. Climate change plays a significant role in worsening the surface urban heat island within the study area.
2. There is a distinct spatiotemporal variation in the urban heat island across the various neighborhoods of Kirkuk City.
3. Modern geospatial technologies play a crucial role in monitoring and mapping the concentration patterns of the urban heat island.

Third: Research Objectives

1. Tracking the evolutionary stages of the urban heat island in Kirkuk City by conducting a comparative analysis of the satellite imagery used in the study for the two time periods, 2008 and 2025.
2. Formulating the necessary strategies to counteract the progression of the urban heat island in Kirkuk City, by adopting sustainable approaches and methods that mitigate the development of this phenomenon.
3. Analyzing the spatiotemporal variations of the urban heat island phenomenon for the years 2008 and 2025 through cartographic modeling, subsequently generating outcomes that can reduce or limit the future exacerbation of this phenomenon.

Fourth: Research Significance

Climate change represents one of the most critical climatological issues of the current century, with its visible impacts manifested primarily through rising global temperatures. The study area is highly susceptible to these climatic shifts, which entail severe negative repercussions, most notably the intensification of the urban heat island phenomenon. This phenomenon, in turn, directly threatens human activities and public health. Consequently, this study acquires its significance by tracking the development of the urban heat island in Kirkuk City, comparing the thermal differentials between 2008 and 2025, and identifying the underlying drivers of its progression within the city.

Fifth: Research Methodology

- **The Historical Approach:** This approach is utilized by geographers to study the evolution of geographical phenomena over time. It involves collecting, organizing, and analyzing historical data to understand how these phenomena were shaped and modified, thereby providing a scientific geographical interpretation of the present reality and linking it to the past. This methodology was applied to study the historical development of the urban heat island phenomenon in Kirkuk City.
- **The Technical Approach:** This approach relies on advanced tools and techniques, such as Geographic Information Systems (GIS) and Remote Sensing, to map and analyze spatial data accurately and objectively. This methodology was employed to interpret the phenomenon and propose practical solutions to the real-world challenges facing Kirkuk City.

Sixth: Scope of the Study Area

- **Spatial Scope:** Geographically, the study area is located in the northern and northeastern sector of Iraq, represented by Kirkuk City. It is bordered to the north by the sub-districts of Shwan and Alton Kupri, and to the south by the sub-districts of Laylan and Taza. To the east, it is bordered by the sub-district of Qarah Hanjir, and to the west by the sub-district of Yaychi. The study area encompasses an overall surface area of (15,803.4) hectares, distributed across (56) residential neighborhoods. Astronomical coordinates place the study area between latitudes (35-21-30) and (35-32-0) North, and longitudes (44-17-30) and (44-28-0) East. Refer to Map (1).
- **Temporal Scope:** This scope is confined to the years 2008 and 2025.

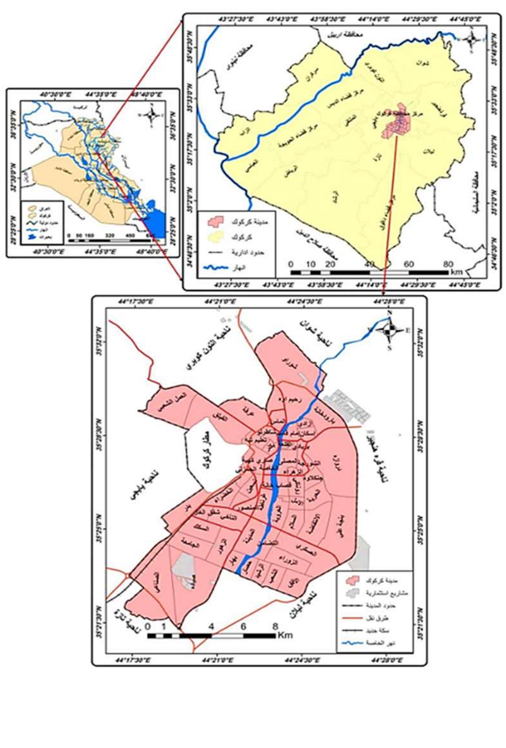

Source: Prepared by the researcher based on: Republic of Iraq, Ministry of Municipalities and Public Works, Directorate General of Urban Planning, Directorate of Urban Planning in Kirkuk; Administrative Map of Iraq, scale 1:1,000,000, utilizing ArcGIS 10.8 software

Section Two: The Concept of Cartographic Modeling and the Requirements and Steps for Deriving Land Surface Temperature (LST)

First: The Concept of Cartographic Modeling

Cartographic modeling is defined as the process of creating a simplified and structured spatial representation of real-world geographical phenomena. Its purpose is to explain, analyze, and comprehend their spatial distribution patterns more accurately and objectively, thereby contributing to the uncovering of spatial relationships and interactions among the components of the studied phenomenon. The concept of the map as a spatial model emerged in the 1960s. The models employed in cartographic modeling vary in their level of complexity; they range from simple models that rely on the theoretical conceptualization of spatial relationships to advanced computer-based models that utilize mathematical and statistical algorithms within Geographic Information Systems (GIS) to analyze spatial phenomena and predict their future behavior (Li & Cheng, 2019, as cited in Ibrahim, 2025, p. 168).

Second: Requirements for Deriving Land Surface Temperature (LST)

1. Satellite Imagery (Landsat):

Satellite imagery constitutes the primary input for building the database of this study. Two generations of this imagery were utilized:

- **The first generation** consists of imagery from Landsat 8, which was launched on February 11, 2013. The satellite's 11 spectral bands are used for multiple purposes. In this study, the visible and near-infrared bands (Bands 4 and 5) are employed to study vegetation cover and extract spectral indices such as the Normalized Difference Vegetation Index (NDVI). Meanwhile, the thermal infrared band (Band 10) is used to estimate Land Surface Temperature (LST) (Department of Science and Technology, n.d., pp. 1–7).
- **The second generation** comprises imagery from Landsat 7, which was launched on April 15, 1999. This satellite features eight spectral bands covering the visible, near-infrared, and thermal infrared spectra. Band 6 is utilized in thermal analysis to derive Land Surface Temperature (LST), while Bands 3 and 4 are used to extract the vegetation index (NDVI) (Al-Suwaidi, 2020, pp. 77-78).

Third: Procedural Steps for Deriving Land Surface Temperature (LST) for the Study Area

1. Calculating Top of Atmosphere (TOA) Spectral Radiance (L):

The process of converting Digital Numbers (DN) of pixels into Top of Atmosphere (TOA) spectral radiance (L) represents the initial practical step in deriving Land Surface Temperature. Raw Digital Numbers cannot be directly utilized in thermal analysis; instead, they must be converted into radiance values that represent the amount of thermal energy recorded at the satellite sensor. This conversion is performed using radiometric calibration coefficients extracted from the metadata file (MTL) accompanying satellite imagery. This transformation is applied to both Landsat 7 and Landsat 8 satellites using the following standard equation (Chander et al., 2009, pp. 893–903):

$$L\lambda = ML \times Q_{cal} + AL$$

Where:

- L: Top of the Atmosphere (TOA) spectral radiance.
- ML: Radiance Multiplicative Factor, extracted from the (MTL) file.
- AL: Radiance Additive Factor, extracted from the (MTL) file.
- Q: Digital Numbers (DN) of the thermal band, representing Band 10 for Landsat 8 and Band 6 for Landsat 7.

2. Calculating Brightness Temperature (BT):

After calculating the TOA spectral radiance (L), it is converted into a Brightness Temperature (BT), which represents the temperature measured at the satellite sensor. This is achieved using specific thermal constants for the thermal band extracted from the metadata file (MTL). This step is fundamental in the LST derivation sequence, as it marks the transitional stage from radiometric values to thermal values. Following the construction of an atmospheric correction model, these values are converted into the brightness temperatures of objects on the Earth's surface according to the following mathematical equation (Chander et al., 2009, pp. 893–903):

$$BT = \frac{k_2}{\ln\left(\frac{K_1}{\boldsymbol{L\lambda}} + 1\right)} - 273.15$$

Where:

- BT: Brightness Temperature degrees Celsius, after subtracting (273.15).
- K1 and K2: Thermal constants extracted from the metadata file (MTL). For Band 6 of Landsat 7, these values are K1 = 666.09 and K2 = 1282.71. For Band 10 of Landsat 8, they are K1 = 774.8853 and K2 = 1321.0789.
- L: Spectral radiance resulting from the first step.
- ln: The natural logarithm.

To obtain the results in degrees Celsius (C), the brightness temperature is converted from Kelvin to Celsius by subtracting the absolute zero offset value, which represents (273.15) Kelvin, from the values generated by the equation.

3. Calculating the Normalized Difference Vegetation Index (NDVI):

Following the derivation of Brightness Temperature (BT), the process advances to calculating the Normalized Difference Vegetation Index (NDVI), which is one of the most vital spectral indices used to estimate vegetation density. The significance of this step lies in its subsequent use to estimate Surface Emissivity, a critical factor for correcting brightness temperature to achieve the final Land Surface Temperature (LST). The calculation of NDVI relies on the visible and near-infrared spectral bands. For Landsat 7, Band 3 (Red) and Band 4 (NIR) were used, whereas for Landsat 8, Band 4 (Red) and Band 5 (NIR) were employed (Rouse et al., 1974, pp. 309-317), according to the following mathematical equation:

$$NDVI = \frac{NIR - Red}{NIR + Red}$$

Where:

- NDVI: Normalized Difference Vegetation Index.
- Red: The Red band.
- {NIR: The Near-Infrared band.

After executing several steps to calculate the NDVI, a series of cartographic models dedicated to the vegetation cover of the study area were prepared for both periods (2008 and 2025) during the summer season, as displayed in Maps (2) and (3).

Map (2): Vegetation Cover Density across Residential Neighborhoods (2008)

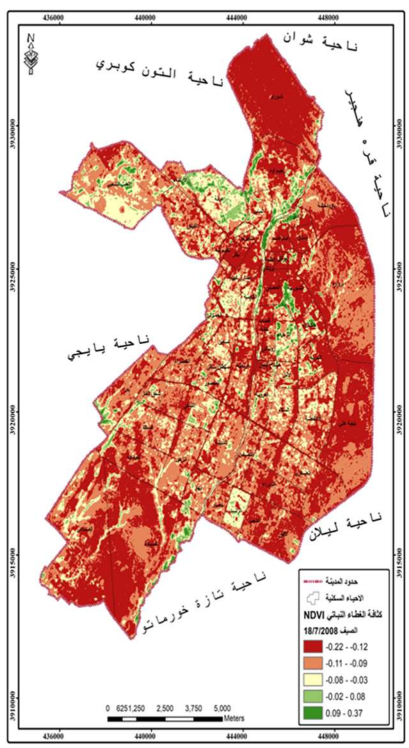

Map (3): Vegetation Cover Density across Residential Neighborhoods (2025)

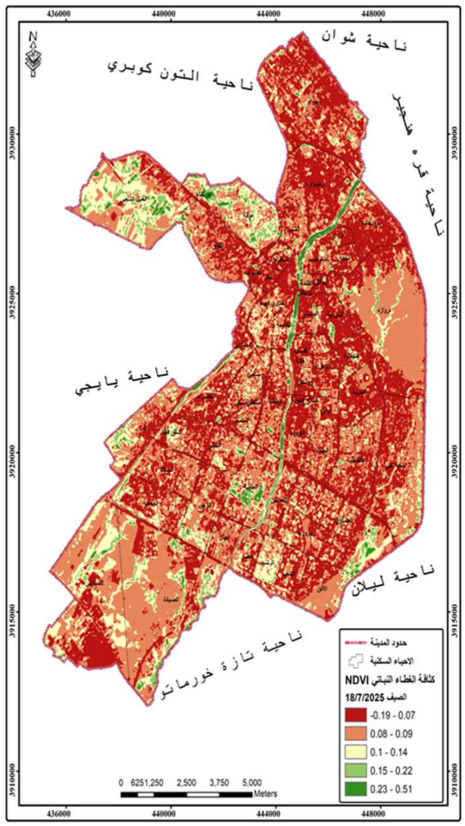

Source: Based on Landsat (7 / 8) satellite data and ArcGIS 10.8 outputs.

4. Calculating the Proportion of Vegetation (Pv):

Remote sensing technologies represent modern and effective means for monitoring the spatiotemporal variations of land cover, particularly vegetation cover, which serves as a critical environmental indicator for detecting land degradation and the expansion of desertification. Vegetation cover is quantitatively expressed using the Normalized Difference Vegetation Index (NDVI), a metric widely utilized to estimate the density and distribution of green canopy (Tucker, 1979, pp. 127-150).

The Proportion of Vegetation (P_v) is defined as the ratio that represents the fractional contribution of green vegetation within a specific surface area unit, derived from NDVI values. This proportion reflects the degree of surface vegetative canopy in terms of both density and vigor (Li et al., 2009, pp. 3801-3853).

Accordingly, a geoprocessing model was designed to calculate the Proportion of Vegetation (P_v) based on the NDVI indices. This was executed by applying normalization followed by squaring operations utilizing the Raster Calculator tool within ArcMap, thereby ensuring the transformation of spectral data into an accurate, quantitative representation of vegetation density, as illustrated in Figure (1-1).

Figure (1): Calculating the Proportion of Vegetation (Pv)

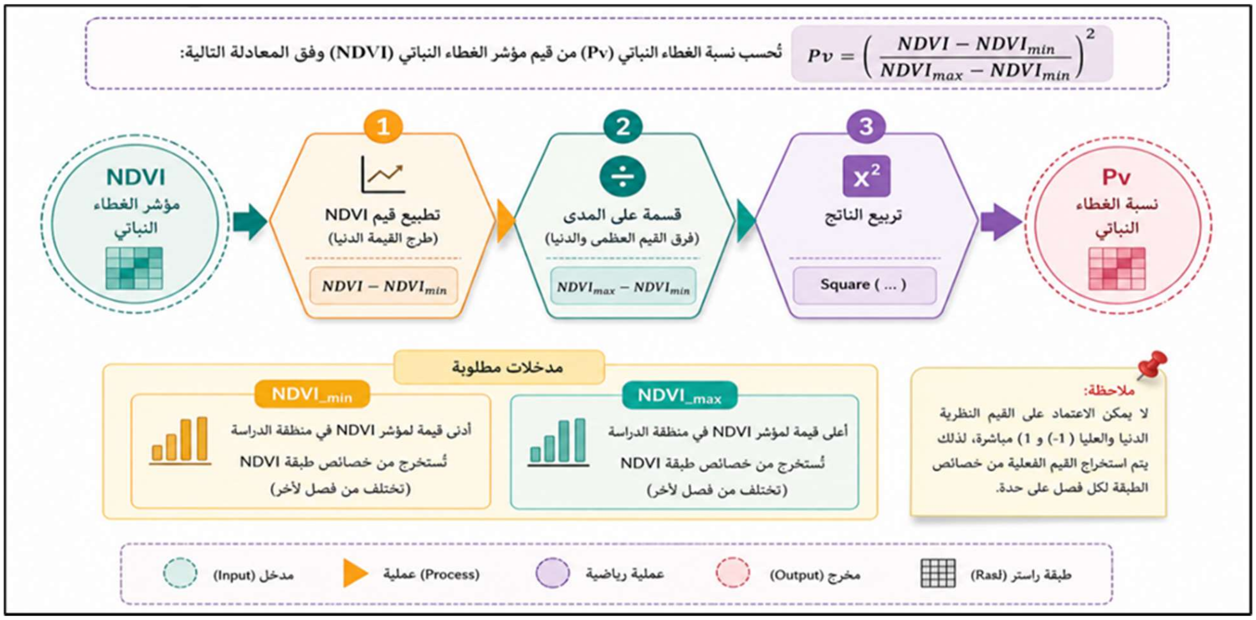

Source: Based on the Model Builder framework.

Consequently, a table has been prepared to represent the vegetation cover area across the residential neighborhoods of the study area during the summer season for the years

2008 and 2025, as presented below in Table (1):

No.	Neighborhood Name	Summer Vegetation 2008 (Hectares)	Summer Vegetation 2025 (Hectares)	No	Neighborhood Name	Summer Vegetation 2008 (Hectares)	Summer Vegetation 2025 (Hectares)
1	Azadi	14.2	2.0	29	Almas	16.3	6.2
2	Iskan	0.6	2.7	30	Al-Madina	9.7	60.7
3	Al-Irtiqaa	14.9	30.7	31	Al-Musalla	4.5	3.0
4	Al-Ufuq	5.3	11.6	32	Al-Mansour	6.8	2.8
5	Al-Amal	6.9	2.9	33	Imam Qasim	12.6	10.1
6	Al-Intifada	14.5	12.2	34	Barood Khana	6.0	8.9
7	Al-Taakhi	29.3	16.5	35	Badr	34.6	36.2
8	Al-Tadhamun	1.3	8.9	36	Beryadi	1.5	0.9
9	Al-Jami'a	16.1	21.9	37	Begler	0.0	0.1

10	Al-Hurriya	14.8	4.1	38	Panja Ali	0.0	34.5
11	Al-Hamzali	18.4	10.7	39	Bahar	12.3	4.1
12	Al-Khassa	14.4	9.1	40	Boulaq	0.1	0.1
13	Al-Khadraa	1.9	21.0	41	Taseen	7.0	8.6
14	Al-Rashid	38.0	18.6	42	Ta'leem Tepe	4.5	1.7
15	Al-Zahraa	50.8	5.1	43	Janqlawa	15.9	6.9
16	Al-Zuhour	9.3	31.2	44	Hisar	1.6	6.6
17	Al-Zawraa	0.6	8.4	45	Darwaza	16.1	38.7
18	Al-Sikak	16.4	8.3	46	Rahim Awa	102.5	14.6
19	Al-Salam	6.0	3.6	47	Runaki	0.6	0.7
20	Al-Sha'ab	1.0	8.3	48	Sultan Saqi	6.0	3.3
21	Al-Shorja	37.3	9.2	49	Shatterlo	2.3	1.6
22	Al-Sina'i	34.0	86.0	50	Gas Flats (Shuqaq Al-Gaz)	8.6	7.7
23	Al-Sayyada	95.8	153.2	51	Shoraw	5.0	29.1
24	Al-Urouba	17.1	2.7	52	Sari Kahya	24.2	12.0
25	Al-Askari	9.2	77.8	53	Salah Al-Din	1.9	0.4
26	Al-Amal Al-Sha'abi	107.4	260.9	54	Arafa	166.2	104.8
27	Al-Fay laq	23.5	17.1	55	Granada	9.9	16.4
28	Al-Qal'a	0.2	1.9	56	Qassab Khana	2.9	3.7
					Total	1078.8	1271.0

Source: Based on Landsat (7-8) satellite data and ArcGIS 10.8 outputs.

The analysis of Table (1) along with Maps (2) and (3) reveals the following observations:

- During the summer season of 2008, the highest vegetation cover area was recorded in Arafa neighborhood, reaching (166.2) hectares, whereas the lowest area was observed in Begler and Panja Ali neighborhoods, registering (0.0) hectares.
- Conversely, the summer season of 2025 recorded the highest vegetation cover area in Al-Amal Al-Sha'abi neighborhood, reaching (260.9) hectares, while the lowest vegetation cover area was noted in Begler and Boulaq neighborhoods, accounting for (0.1) hectares.

5. Calculating Land Surface Emissivity (LSE):

Land Surface Emissivity is a critical physical variable in deriving Land Surface Temperature (LST), as it expresses the surface's capacity to emit thermal energy relative to a blackbody. Emissivity values vary according to the nature of land cover; they are relatively high in areas with dense vegetation cover, whereas they fluctuate across bare and semi-arid lands due to variations in soil characteristics, rock types, and surface moisture. Consequently, brightness temperature is not directly adopted as the definitive land surface temperature; instead, it is subsequently corrected using land surface emissivity to obtain more realistic and precise values. In this study, land surface emissivity was estimated based on the proportion of vegetation (Pv) using the following equation (Wubet, 2003, p. 14):

$$\varepsilon = 0.004 \times Pv + 0.986$$

6. Calculating Land Surface Temperature (LST):

This step represents the final stage in deriving land surface temperature. Brightness Temperature (BT) is insufficient on its own to express the actual temperature of the surface, as it merely represents the thermal response recorded at the satellite sensor. Therefore, it is corrected based on Land Surface Emissivity, which reflects the characteristics of land cover and its capacity to emit thermal energy (Wubet, 2003, p. 16).

At this stage, a comprehensive geoprocessing model was constructed within the ArcMap environment utilizing Model Builder. This model integrates the outputs of all preceding stages—namely, spectral radiance, brightness temperature, the normalized difference vegetation index, the proportion of vegetation, and land surface emissivity—ultimately generating the final Land Surface Temperature (LST) layer, as shown in Figure (2). This model is applied to both Landsat 7 and Landsat 8 imagery using the same mechanism, while accounting for the differences in bands and thermal constants specific to each satellite, in accordance with the following equation (Avdan & Jovanovska, 2016, p. 6):

$$LST = \frac{BT}{1 + \left(\frac{0.00115 \times BT}{1.4388}\right) \times \ln(\varepsilon)}$$

Figure (2): The Final Model for Deriving Land Surface Temperature (LST)

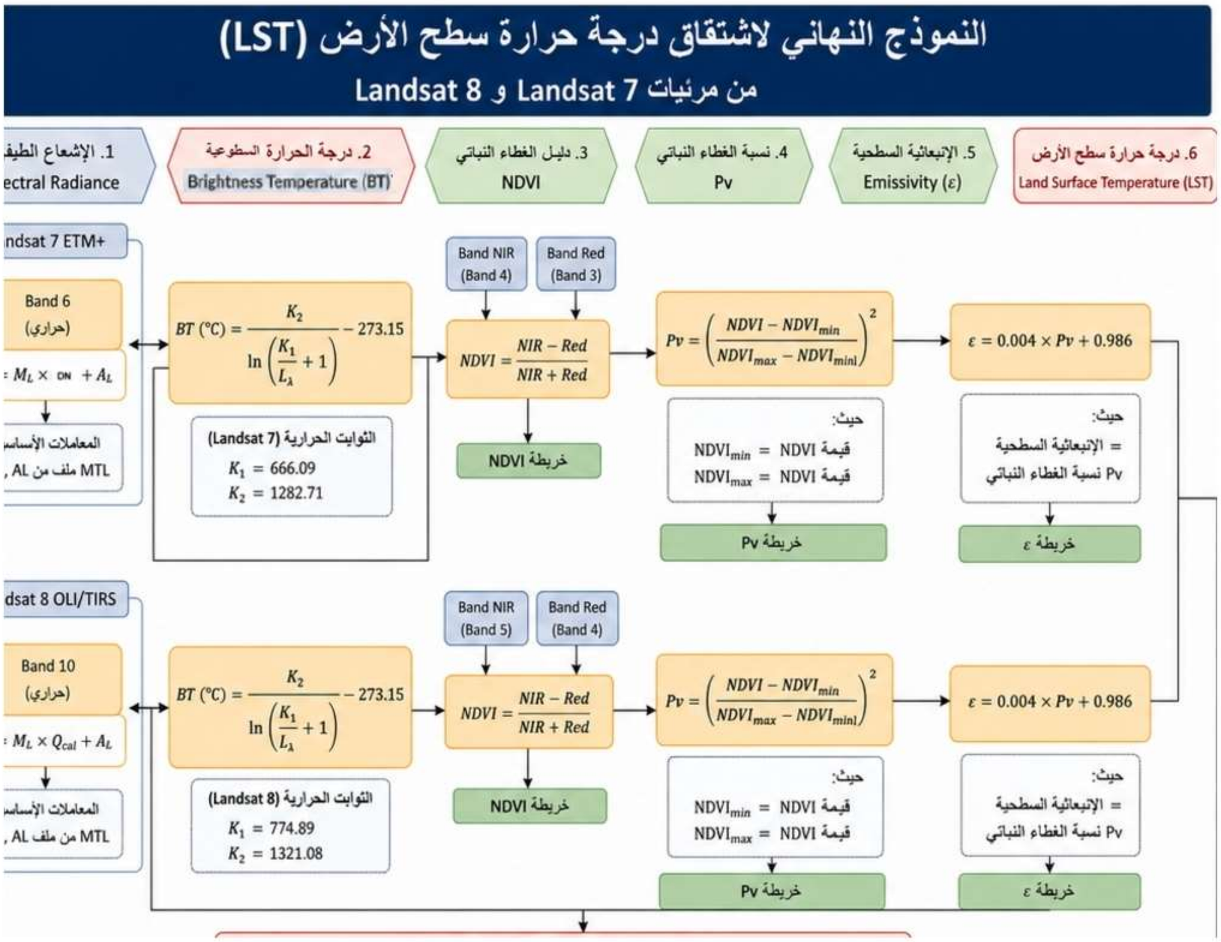

Source: Based on the Model Builder framework.

Section Three: Spatiotemporal Analysis of the Final Summer Surface Urban Heat Island (SUHI/LST) Models within the Study Area

Following the derivation process of Land Surface Temperatures (LST) utilizing Landsat (7 and 8) satellite imagery and ArcGIS software, a specialized dataset representing the surface temperatures across the residential neighborhoods of Kirkuk City was generated. Furthermore, cartographic models were constructed for both periods (2008–2025) during the summer season, as presented below in Table (2) and Maps (4) and (5).

Table (2): Land Surface Temperatures (LST) across Residential Neighborhoods within the Study Area during the Summer Season (2008 and 2025)

No.	Neighborhood Name	Summer 2008(C) - Mean	Summer 2008(C) - Max	Summer 2008(C)Min	Summer 2025 Mean	Summer 2025(C) - Max	Summer 2025(C) - Min
1	Azadi	31.6	35	27	44.4	47	42
2	Iskan	32.4	36	30	45.4	49	42
3	Al-Irtiqaa	31	36	24	45.4	50	41
4	Al-Ufuq	34	37	29	47	51	44
5	Al-Amal	32.7	35	30	46.4	49	43
6	Al-Intifada	32.9	36	30	45.6	50	43
7	Al-Taakhi	33	37	29	47	50	43
8	Al-Tadhamun	32.8	35	30	45.3	48	43
9	Al-Jami'a	32.6	36	28	47.1	50	44
10	Al-Hurriya	32.7	36	29	46.5	51	43
11	Al-Hamzali	33.2	36	30	47.3	50	44
12	Al-Khassa	32.4	35	29	43.4	48	39
13	Al-Khadraa	33.1	36	30	46.9	50	44
14	Al-Rashid	32.3	37	29	45.4	47	43
15	Al-Zahraa	32	36	28	46.2	50	43
16	Al-Zuhour	33.2	36	30	47.8	52	44
17	Al-Zawraa	33.7	37	31	46.3	50	43
18	Al-Sikak	32.9	36	30	46.7	49	44
19	Al-Salam	32.9	36	30	45.5	48	43
20	Al-Sha'ab	34	38	31	46.6	49	44
21	Al-Shorja	31.5	35	27	44.9	48	42
22	Al-Sina'i	33.3	37	29	46.3	52	39
23	Al-Sayyada	31.9	37	24	45.8	52	38
24	Al-Urouba	32.9	36	30	45.6	49	42
25	Al-Askari	33.3	37	29	45.2	50	38
26	Al-Amal Al-Sha'abi	32.4	37	27	44.1	55	38
27	Al-Fay laq	33.4	37	28	47.4	52	43
28	Al-Qal'a	32.9	35	31	47.6	52	43
29	Almas	31.7	35	29	45.7	49	43
30	Al-Madina	33.4	36	30	44.8	51	40
31	Al-Musalla	31.9	35	27	44.9	48	42

32	Al-Mansour	31.7	35	29	46.2	48	44
33	Imam Qasim	30.8	34	27	43.5	48	39
34	Barood Khana	33.8	36	30	44.9	51	39
35	Badr	31.8	36	25	46.9	50	43
36	Beryadi	32	34	30	45.7	48	43
37	Begler	32.1	34	30	45.1	46	43
38	Panja Ali	35.2	37	32	46.7	50	43
39	Bahar	32	35	26	46.9	50	44
40	Boulaq	32.1	34	31	46.8	49	44
41	Taseen	32.2	36	29	46.2	49	44
42	Ta'leem Tepe	32.6	35	30	44.9	47	43
43	Janqlawa	33.6	35	28	46.4	51	44
44	Hisar	35.6	37	30	46.3	49	43
45	Darwaza	31.9	50	30	48.3	53	40
46	Rahim Awa	32.4	37	26	45.6	52	44
47	Runaki	32.3	34	30	46.7	48	44
48	Sultan Saqi	32.6	35	29	44.7	49	42
49	Shatterlo	31.6	33	30	46.7	46	44
50	Gas Flats (Shuqaq Al-Gaz)	33	35	30	47	49	42
51	Shoraw	33.8	37	29	47	51	42
52	Sari Kahya	32.3	36	29	45.5	48	42
53	Salah Al-Din	32.6	34	30	46.5	48	44
54	Arafa	32	36	28	46.8	52	42
55	Granada	32.4	36	29	46.1	50	43
56	Qassab Khana	32.9	36	31	44.8	50	41
	Total	1828.8	2016	1623	2575.9	2778	2374

Source: Based on Landsat (7/8) satellite data and ArcGIS 10.8 outputs.

The spatial analysis of Table (2) and Maps (4) and (5) for the summer seasons of 2008 and 2025 reveals that the Surface Urban Heat Island (SUHI) is primarily concentrated along the outskirts of Kirkuk City. This distribution is verified by the statistical indicators in the dataset—representing the mean, maximum, and minimum temperatures—as well as the cartographic color ramp, which progresses from dark brown for the highest thermal zones to yellow for the lowest temperature areas.

In the summer of 2008, the SUHI effect was predominantly concentrated in the eastern and southern sectors of the study area. This zone encompassed several areas, most notably the Darwaza neighborhood, which recorded the highest maximum temperature at (50 C), whereas the lowest minimum temperatures were observed in Al-Irtiqaa and Al-Sayyada neighborhoods, dropping to (24 C).

Conversely, during the summer season of 2025, the SUHI exhibited significant peripheral expansion, engulfing new residential sectors and open lands. The thermal anomaly extended across almost all geographic orientations of the city, except for the western sector, where the heat island's intensity remained relatively low. During this period, Al-Amal Al-Sha'abi neighborhood recorded the highest maximum temperature at (55.C), while Al-Sayyada, Al-Askari, and Al-Amal Al-Sha'abi neighborhoods represented the lowest thermal thresholds, registering a minimum of (38.C).

The spatial concentration of heat islands in these specific sectors is attributed to localized environmental and anthropogenic factors. Chief among these is the proximity to the "Eternal Fire" gas flares operated by the North Oil Company, alongside the presence of prominent topographic terrain in the northern and eastern sectors. These topographic barriers obstruct the prevailing easterly and northerly winds from mitigating temperatures in the adjacent urban zones. This is further exacerbated by rapid urban expansion occurring at the expense of agricultural land, particularly along the southern outskirts of the study area.

Furthermore, the cumulative spatial aggregates of the maximum, minimum, and mean values across the residential units indicate that urban temperatures in 2008 were systematically lower than those recorded in 2025. In conclusion, the synergistic effects of macro-climate change, horizontal urban sprawl, horizontal decline in vegetation cover, complex local topography, and industrial thermal emissions from the "Eternal Fire" have collectively intensified the SUHI dynamics within the study area. This intense thermal footprint on the city's periphery poses a high risk of expanding into the inner urban core in the near future unless sustainable mitigation strategies are actively implemented.

Map (4): Land Surface Temperatures (LST) for the Summer Season (2008)

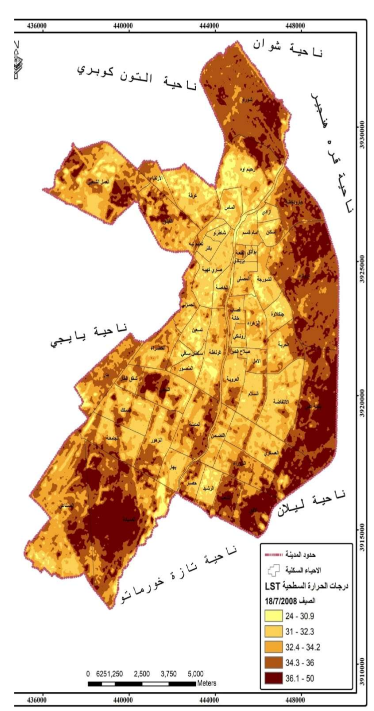

Map (5): Land Surface Temperatures (LST) for the Summer Season (2025)

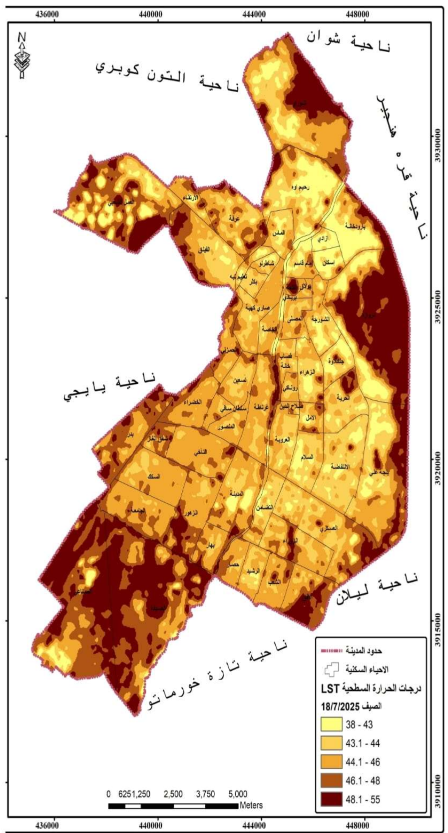

Source: Based on Landsat (7/8) satellite data and ArcGIS 10.8 outputs.

First: Conclusions

1. Utilizing satellite imagery, the study demonstrated that the Surface Urban Heat Island (SUHI) in Kirkuk City is primarily located along its outskirts. During the summer season of 2008, the highest concentration of heat islands was centered in the eastern and southern sectors. However, by 2025, the phenomenon expanded substantially, covering most geographic orientations of the city alongside scattered urban pockets within the interior core.
2. The Darwaza and Al-Amal Al-Sha'abi neighborhoods emerged as the zones recording the highest thermal thresholds. This sharp thermal anomaly is strongly attributed to the proximity to the industrial gas flares known as the "Eternal Fire" in those sectors, as well as the presence of prominent topographic terrain along the eastern and northern borders of the study area.
3. The study illustrated that the SUHI intensity in Kirkuk City significantly intensified during the summer of 2025 compared to 2008. This escalation is directly caused by rapid horizontal urban expansion, the acute decline in vegetation cover, and the compounding effects of macro-climate change, which collectively exacerbated the urban heat island dynamics.
4. The spatial aggregates of the maximum, minimum, and mean temperature values across the residential neighborhoods indicate that urban surface temperatures in 2008 were systematically

lower than those recorded in 2025. This temporal upward shift is driven by ongoing climate change trends coupled with the continuous growth of anthropogeographic activities previously discussed.

Second: Recommendations

1. Continuous integration of remote sensing (RS) technologies and Geographic Information Systems (GIS) should be adopted to monitor environmental and thermal variations within Kirkuk City. These advanced tools offer high-precision capabilities to track the spatiotemporal evolution of urban heat islands, thereby providing critical geospatial data to support sustainable urban planning and institutional decision-making.
2. Immediate priority must be directed toward mitigating the heat island intensity along the urban periphery of Kirkuk City—specifically in the eastern, northern, and southern sectors which recorded the most severe thermal concentrations. This should be achieved by scaling up urban green infrastructure, maximizing vegetative canopies, and establishing strategic green buffer zones designed to lower land surface temperatures and enhance the urban microclimate.
3. Seasonal mitigation programs must be formulated to alleviate the adverse effects of the summer heat island. These frameworks should prioritize extensive urban afforestation, the expansion of shaded public spaces, and the enforcement of high-albedo building materials and cool roofing technologies to minimize the absorption and retention of solar radiation.

References:

1- Ibrahim, Saad Thamer. (2025). *Cartographic modeling of the thermal island in Erbil city* (Unpublished doctoral dissertation). College of Arts, Tikrit University, Iraq.

2- Al-Suwaidi, M. A. (2020). *The use of geographic information systems in classifying remote sensing data*: A comparative study. University of Babylon

Journal of Human Sciences, 28(6) ,96-74.

3. Chander, G., Markham, B. L., & Helder, D. L. (2009). *Summary of current radiometric calibration coefficients for Landsat MSS, TM, ETM+, and EO-1 ALI sensors. Remote Sensing of Environment, 113(5), 893–903.*

4-Avdan, U., & Jovanovska, G. (2016). *Algorithm for automated mapping of land surface temperature using Landsat 8 satellite data.* Journal of Sensors, 2016, 1–8.

5- Department of Science and Technology, Ministry of Science and Technology, *Government of India. (n.d.). Calculate brightness temperature using Landsat-8 using SAGA GIS (IGET_SA_004). IGET Geospatial Education Portal.*

6- Li, Z. L., Tang, R., Wan, Z., Bi, Y., Zhou, C., Tang, B., Yan, G., & Zhang, X. (2009). *A review of current methodologies for regional evapotranspiration estimation from remotely sensed.*

7- Rouse, J. W., Haas, R. H., Schell, J. A., & Deering, D. W. (1974). *Monitoring vegetation systems in the Great Plains with ERTS. In Proceedings of the Third Earth Resources Technology Satellite-1 Symposium (NASA SP-351, Vol*

8- Tucker, C. J. (1979). *Red and photographic infrared linear combinations for monitoring vegetation,Remote Sensing of Environment, Washington, DC: NASA 8(2), 127–150.*

9- Wubet, M. T. (2003). *Estimation of absolute surface temperature by satellite remote sensing (Master's thesis, International Institute for Geo-Information Science and Earth Observation).* Enschede, The Netherlands.